University of Cape Town Mathematics Honours Thesis:
Sharp Sobolev Constants - a Numerical Investigation

Stefan Juhnke
JHNSTE014
Thesis Supervisor: Dr Jesse Ratzkin

November 15, 2013

Abstract

After a development of theoretical underpinnings and an analysis of the literature on numerical algorithms, a generalised eigenvalue equation relating to the sharp Sobolev constant was solved numerically on a number of domains. The aim was to gather numerical evidence for a conjecture concerning the distribution functions of the solutions. All results obtained support the conjecture, calling for further work to generalise the solutions over certain parameter values and over more complex domains.

Contents

1 Introduction

Two important constants that relate to the geometry of a bounded domain in the plane are torsional rigidity and principal frequency. The best constant in the Sobolev inequality for a bounded domain in $\mathbb{R}^n$ allows for a generalisation of the concepts of torsional rigidity and principal frequency for different parameter values as well as an extension into higher dimensions. These generalisations will be the subject of this report, with an attempt at starting to answer one of the questions that is still open in this field.

Ω will be used to denote a bounded domain in $\mathbb{R}^n$ with a piecewise Lipshitz boundary $\partial\Omega$ which satisfies a uniform cone condition both on its interior and exterior. Let x denote the Cartesian coordinates $(x_1, x_2, ...x_n)$, while dx denotes the usual Cartesian differentials $dx_1 dx_2 ... dx_n$ and $d\theta$ the surface differential on a hypersurface $\Sigma \subset \mathbb{R}^n$.

The Constant $C_p(\Omega)$

For each $p \geq 1$ for $n = 2$ and $1 \leq p < \frac{2n}{n-2}$ for $n \geq 3$, let $C_p(\Omega)$ be defined by

$$C_p(\Omega) = \inf \left\{ \phi_p(u) = \frac{\int_\Omega |\nabla u(x)|^2 dx}{\left(\int_\Omega u(x)^p dx \right)^{\frac{2}{p}}} \Big| u \in L^p(\Omega) \cap W_0^{1,2}(\Omega), u \not\equiv 0 \right\}$$

It will be shown below that this infimum is both finite and that it is achieved by a positive function. For $p = 1$, $C_1(\Omega) = \frac{4}{P(\Omega)}$ where $P(\Omega)$ is the torsional rigidity of the domain, while for $p = 2$ we get the principal frequency $C_2(\Omega) = \lambda(\Omega)$ (see [2]). In general, $C_p(\Omega)$ is the squared reciprocal of the sharp Sobolev constant, and is a topic of much current research. A large part of this report will be devoted to finding functions that achieve this infimum for different domains and different values of p. The problem of finding these functions is equivalent to solving

$$\Delta u + \Lambda u^{p-1} = 0 \quad \text{subject to} \quad u\big|_{\partial\Omega} = 0; \quad u \geq 0, u \not\equiv 0 \tag{1}$$

for some positive constant Λ, since this is the Euler-Lagrange equation (9) relevant to the variational problem of minimizing the functional $\phi_p(u)$. The additional specification $u \geq 0$ is discussed in section 4.

We will need the following definition of a distribution function

Distribution Function $\mu_{p,\Omega}(t)$

Given a positive solution u on a domain Ω normalised such that $0 \leq u \leq 1$, define the distribution function

$$\mu_{p,\Omega}(t) = \text{Vol}(\{x \in \Omega | u(x) \geq t\}).$$

The report will focus on how the distribution function for the solution as well as the values of $C_p(\Omega)$ change with different values of p, based on numerical solution of the Euler-Lagrange equation.

A numerical algorithm based on that of Li and Zhou [7] was implemented to solve (1). These numerical solutions were then used to calculate the distribution functions as well as the constants $C_p(\Omega)$ for different values of p. The algorithm fails to work for $1 < p < 2$ but gives numerically verifiable results in all other cases.

A specific conjecture about the distribution function, namely that

$$p < q \Rightarrow \mu_{p,\Omega}(t) \geq \mu_{q,\Omega}(t) \; \forall t \in [0, 1],$$

was proposed by thesis supervisor Dr Jesse Ratzkin. The numerical results provide compelling evidence in favour of the conjecture on the domains investigated.

Before going on to describe the algorithm for a numerical solution and presenting the results, we will develop some of the theory alluded to in this introduction.

2 Sobolev Imbedding Theorem

Of critical importance to the discussion of this report will be the Sobolev Imbedding Theorem.

Several relevant definitions and requisite results follow.

2.1 Definitions

Multi-index

A multi-index α is defined as $\alpha = (\alpha_1, ..., \alpha_n) \in \mathbb{N}_0^n$, $\mathbb{N}_0 := \mathbb{N} \cup \{0\}$, with $|\alpha| = \alpha_1 + ... + \alpha_n \in \mathbb{N}_0$. This allows us to write

$$D^\alpha \phi(x) := \frac{\partial^{|\alpha|}}{\partial x^{\alpha_1} ... \partial x^{\alpha_n}} \phi(x).$$

Weak Derivative:

Let u be locally integrable in the domain Ω and α any multi-index. A locally integrable function v is called the α^{th} weak derivative of u if it satisfies

$$\int_\Omega \phi(x) v(x) dx = (-1)^{|\alpha|} \int_\Omega u(x) D^\alpha \phi(x) dx \quad \text{for all } \phi \in C_0^{|\alpha|}(\Omega)$$

where $C_0^k(\Omega)$ is the set of functions with compact support in Ω all of whose derivatives of order $\leq k$ are continuous in Ω.

We now denote the space of k times weakly differentiable functions $W^k(\Omega)$.

The $W^{k,p}$ Sobolev Spaces

The Sobolev Banach spaces are then defined as follows:

$$W^{k,p}(\Omega) = \{u \in W^k(\Omega) | D^\alpha u \in L^p(\Omega) \text{ for all } |\alpha| \leq k\}.$$

Here $L^p(\Omega)$ denotes the Lebesgue space defined by

$$L^p(\Omega) = \{u | \int_\Omega |u(x)|^p dx < \infty\} \quad \text{for } 1 \leq p < \infty.$$

The Sobolev norm is given by

$$\|f\|_{W^{k,p}} := \|f\|_{k,p,\Omega} := \Big(\sum_{|\alpha| \leq k} \int_\Omega |D^\alpha f(x)|^p dx \Big)^{\frac{1}{p}}.$$

When the Sobolev space has compact support in Ω this is denoted $W_0^{k,p}$.

Bounded Linear Operators

A linear operator $T : X \to Y$ between two normed linear spaces X and Y with norms $\| \cdot \|_X$ and $\| \cdot \|_Y$ is said to be bounded if there exists a constant $M > 0$ such that $\|Tx\|_Y \leq M \|x\|_X$ for all $x \in X$.

Continuous Embedding of Banach Spaces

A Banach space $\mathcal{B}_1$ is continuously embedded in a Banach space $\mathcal{B}_2$ (in symbols: $\mathcal{B}_1 \hookrightarrow \mathcal{B}_2$) if there exists a bounded, linear and injective mapping $\mathcal{B}_1 \to \mathcal{B}_2$.

2.2 Results

Generalised Hölder Inequality

For $m \in \mathbb{N}, m \geq 2$ and exponents $p_1, ..., p_m \in (1, \infty)$ where $p_1^{-1} + ... + p_m^{-1} = 1$, it is true that

$$\int_\Omega |f_1(x)...f_m(x)|dx \leq \|f_1\|_{L^{p_1}(\Omega)}...\|f_m\|_{L^{p_m}(\Omega)},$$

for all $f_j \in L^{p_j}(\Omega)$ with $j = 1, ..., m$. This follows from Hölder's inequality by induction.

Density of $C_0^\infty(\Omega)$ in $W_0^{1,2}(\Omega)$ and $L^p(\Omega)$

Here and elsewhere it will be useful to note that $C_0^\infty(\Omega)$ is dense in both $W_0^{1,2}(\Omega)$ and $L^p(\Omega)$ (see Gilbarg and Trudinger [6] section 7.6).

2.3 Statement and Proof of Sobolev Embedding Theorem

Theorem 2.3.1. *For $1 \leq p < n$, $W_0^{1,p}(\Omega)$ is continuously embedded in $L^{\frac{np}{n-p}}$ with a constant $C = C(n, p) \in (0, \infty)$ such that, for any $u \in W_0^{1,p}(\Omega)$,*

$$\|u\|_{\frac{np}{n-p}} \leq C\|Du\|_p. \tag{2}$$

The proof is given based on its presentation in [11]:

Proof. We start with the case $p = 1$ and the space $C_0^\infty(\Omega)$ which is a dense subspace of $W_0^{1,p}$. We can represent any $C_0^\infty(\Omega)$ by

$$u(x) = \int_{-\infty}^{x_i} D_i u(x)dx_i$$

and we therefore have that

$$|u(x)| \leq \int_{-\infty}^{x_i} |D_i u(x)|dx_i \leq \int_{-\infty}^{\infty} |D_i u(x)|dx_i.$$

Multiplying the inequality over all i and taking both sides to the power of $\frac{1}{n-1}$ gives

$$|u(x)|^{\frac{n}{n-1}} \leq \left(\prod_{i=1}^{n} \int_{-\infty}^{\infty} |D_i u(x)|dx_i\right)^{\frac{1}{n-1}}.$$

If we integrate the above with respect to any x_j and apply the generalized Hölder inequality we obtain

$$\begin{aligned}\int_{-\infty}^{\infty} |u(x)|^{\frac{n}{n-1}} dx_j &\leq \left(\int_{-\infty}^{\infty} |D_j u(x)|dx_j\right)^{\frac{1}{n-1}} \int_{-\infty}^{\infty} \prod_{i=1,...,n;i\neq j} \left(\int_{-\infty}^{\infty} |D_i u(x)|dx_i\right)^{\frac{1}{n-1}} dx_j \\ &\leq \left(\int_{-\infty}^{\infty} |D_j u(x)|dx_j\right)^{\frac{1}{n-1}} \prod_{i=1,...,n;i\neq j} \left(\int_{-\infty}^{\infty}\int_{-\infty}^{\infty} |D_i u(x)|dx_i dx_j\right)^{\frac{1}{n-1}}.\end{aligned}$$

Integrating over all x_j then gives

$$\int_{\mathbb{R}^n} |u(x)|^{\frac{n}{n-1}} dx = \left(\|u\|_{\frac{n}{n-1}}\right)^{\frac{n-1}{n}} \leq \left(\prod_{i=1}^{n} \int_{\mathbb{R}^n} |D_i u(x)|dx\right)^{\frac{1}{n-1}}.$$

Raising both sides to the power of $\frac{n}{n-1}$, we then have that

$$\begin{aligned}
\|u\|_{\frac{n}{n-1}} &\leq \left(\prod_{i=1}^{n} \int_{\mathbb{R}^n} |D_i u(x)| dx \right)^{\frac{1}{n}} \\
&\leq \frac{1}{n} \int_{\Omega} \left(\sum_{i=1}^{n} |D_i u(x)| \right) dx \quad \text{by convexity} \\
&\leq \frac{1}{\sqrt{n}} \int_{\Omega} |Du(x)| dx \\
&\leq \frac{1}{\sqrt{n}} \|Du\|_1 \qquad (3)
\end{aligned}$$

for all $C_0^\infty(\Omega)$. We can now extend this to the cases $1 \leq p < n$ by replacing u in (3) by $|u|^\gamma$ for $\gamma > 1$ and using Hölder's inequality

$$\begin{aligned}
\||u|^\gamma\|_{\frac{n}{n-1}} &\leq \frac{1}{\sqrt{n}} \int_{\Omega} \big| D|u(x)|^\gamma \big| dx \\
&= \frac{\gamma}{\sqrt{n}} \int_{\Omega} |u(x)|^{\gamma-1} |Du(x)| dx \\
&\leq \frac{\gamma}{\sqrt{n}} \||u(x)|^{\gamma-1}\|_q \|Du\|_p
\end{aligned}$$

where q and p are conjugate exponents. This gives

$$\|u\|^\gamma_{\frac{\gamma n}{n-1}} \leq \frac{\gamma}{\sqrt{n}} \|u\|^{\gamma-1}_{q(\gamma-1)} \|Du\|_p$$

In order to divide the two norms involving u, we require $\frac{\gamma n}{n-1} = (\gamma-1)q = (\gamma-1)\frac{p}{p-1}$, i.e. $\gamma = \frac{np-p}{n-p}$, giving

$$\|u\|_{\frac{np}{n-p}} \leq \frac{np-p}{\sqrt{n}(n-p)} \|Du\|_p \text{ for all } u \in C_0^1(\Omega).$$

The result follows for the space $C_0^\infty(\Omega)$ with the constant $C = \frac{np-p}{\sqrt{n}(n-p)}$. To extend the result to $u \in W_0^{1,p}$, we let u_m be a sequence of $C_0^\infty(\Omega)$ functions tending to u in $W_0^{1,p}$. We apply the estimates in (2) to the differences $u_{m_1} - u_{m_2}$ and find that u_m is a Cauchy sequence in $L^{\frac{np}{n-p}}(\Omega)$. Since this is a Banach space we have that $u \in L^{\frac{np}{n-p}}(\Omega)$. □

3 Rellich-Kondrachov Compactness Theorem

The Rellich-Kondrachov Compactness Theorem will be used in conjunction with the Sobolev Imbedding Theorem to allow us to deduce that the constant $C_p(\Omega)$ is finite and realised by a positive function. Again, let us first list a number of definitions and results.

3.1 Definitions

Compact Imbedding of Banach Spaces

Let $\mathcal{B}_1$ be a Banach space that is continuously embedded in a Banach space $\mathcal{B}_2$. Then $\mathcal{B}_1$ is compactly imbedded in $\mathcal{B}_2$ if the imbedding operator $I : \mathcal{B}_1 \to \mathcal{B}_2$ is compact, i.e. if the images of the bounded sets in $\mathcal{B}_1$ are precompact in $\mathcal{B}_2$. Here, a set A is called precompact if each sequence $\{f_k\}_{k=1}^\infty \subset A$ contains a subsequence converging in $\mathcal{B}_2$ with respect to the norm on $\mathcal{B}_2$.

$L^p_{loc}(\Omega)$ Spaces

Let $L^p_{loc}(\Omega)$ denote the linear space of measurable functions locally p-integrable in Ω. The $L^p_{loc}(\Omega)$ are topologized as follows: A sequence $\{u_m\}$ converges to u in the sense of $L^p_{loc}(\Omega)$ if $\{u_m\}$ converges to u in $L^p(\Omega')$ for each $\Omega' \subset\subset \Omega$.

Mollifiers

A mollifier ρ is a non-negative function in $C^\infty(\mathbb{R}^n)$ that vanishes outside the unit ball $B_1(0)$ and satisfies $\int \rho dx = 1$. A typical example is

$$\rho(x) = \begin{cases} c \exp\left(\frac{1}{|x|^2-1}\right), & \text{for } |x| \leq 1. \\ 0, & \text{for } |x| \geq 1, \end{cases} \tag{4}$$

where c is chosen such that $\int \rho dx = 1$.

Regularisation and Approximation by Smooth Functions

For $u \in L^p_{loc}(\Omega)$ and $h > 0$, the regularisation of u, denoted by u_h, is then defined by the convolution

$$u_h(x) = h^{-n} \int_\Omega \rho\left(\frac{x-y}{h}\right) u(y) dy \tag{5}$$

provided $h < \text{dist}(x, \partial\Omega)$. Then u_h belongs to $C^\infty(\Omega')$ for any $\Omega' \subset\subset \Omega$ provided $h < \text{dist}(x, \partial\Omega)$. Furthermore, if u belongs to $L^1(\Omega)$, then u_h lies in $C^\infty_0(\mathbb{R}^n)$ for arbitrary $h > 0$. The signifant feature of this regularisation is that if $u \in C^0(\Omega)$, then u_h converges uniformly to u as h tends to zero on any domain $\Omega' \subset\subset \Omega$ (see Gilbarg and Trudinger [6] section 7.2).

Equicontinuity

Let X and Y be metric spaces. A family $\mathcal{F}$ of functions mapping X to Y is said to be equicontinuous if for every $\varepsilon > 0$ there exists a $\delta > 0$ such that

$$d_X(x_1, x_2) < \delta \Rightarrow d_Y(f(x_1), f(x_2)) < \varepsilon \ \ \forall f \in \mathcal{F}. \tag{6}$$

3.2 Results

Arzela-Ascoli Theorem

Let X be a separable metric space and $\mathcal{F}$ be a family of equicontinuous functions mapping X onto $\mathbb{R}$. If there exists a mapping $M : X \to \mathbb{R}^+$ such that $|f(x)| \leq M(x)$ for all $f \in \mathcal{F}$, then every sequence $\{f_n\} \in \mathcal{F}$ has a subsequence $\{f_{n_k}\}$ which converges uniformly on all compact subsets of X (i.e. $\mathcal{F}$ is precompact).

A Result obtained from Hölder's Inequality

A useful consequence of Hölder's inequality is that for $u \in L^r(\Omega) \cap L^q(\Omega) \cap L^p(\Omega)$ we have

$$\|u\|_q \leq \|u\|_p^\lambda \|u\|_r^{1-\lambda} \tag{7}$$

where $p \leq q \leq r$ and $\frac{1}{q} = \frac{\lambda}{p} + \frac{1-\lambda}{r}$.

3.3 Statement and Proof of Rellich-Kondrachov Compactness Theorem

Theorem 3.3.1. *The spaces $W_0^{1,p}(\Omega)$ are compactly imbedded in the spaces L^q for any $q < \frac{np}{n-p}$ if $p < n$.*

The proof is given based on its presentation in [11]:

Proof. Let us start with a bounded set

$$\mathcal{K} := \left\{ f \in W_0^{1,p}(\Omega) \cap L^q(\Omega) : \|f\|_{1,p,\Omega} \leq s \right\} \subset L^q(\Omega)$$

and let us take an arbitrary sequence $\{f_k\}_{k=1}^{\infty} \subset \mathcal{K}$. Then we can find a sequence $\{g_k\}_{k=1}^{\infty} \subset C_0^{\infty}(\Omega)$ with the property

$$\|g_k - f_k\|_{1,p,\Omega} \leq \frac{1}{k}, \tag{8}$$

where we have that $\|g_k - f_k\|_{1,p,\Omega} \leq 1 + s$ for all $k \in \mathbb{N}$.
We will now show that we can select a convergent subsequence from $\{g_{k_l}\}_{l=0}^{\infty} \subset \{g_k\}_{k=1}^{\infty}$.

Take an arbitrary $\varepsilon \in (0, 1]$ and consider the sequence of functions

$$g_{k,\varepsilon}(x) := \frac{1}{\varepsilon^n} \int_{\mathbb{R}^n} \rho\left(\frac{x-y}{\varepsilon}\right) g_k(y) dy = \int_{\mathbb{R}^n} \rho(z) g_k(x - \varepsilon z) dz \in C_0^{\infty}(\Theta)$$

with

$$\Theta := \{x \in \mathbb{R}^n : dist(x, \Omega) < 1\}.$$

For each fixed $\varepsilon \in (0.1]$ the sequence of functions $\{g_{k,\varepsilon}\}_{k=1}^{\infty}$ is uniformly bounded and equicontinuous by the following estimates for all $x \in \Theta$:

$$|g_{k,\varepsilon}(x)| \leq \frac{1}{\varepsilon^n} \rho\left(\frac{x-y}{\varepsilon}\right) |g_k(y)| dy \leq \frac{C_0}{\varepsilon^n} \sup_{|z| \leq 1} \rho(z)$$

and

$$\begin{aligned} |Dg_{k,\varepsilon(x)}| &\leq \frac{1}{\varepsilon^{n+1}} \int_{\mathbb{R}^n} \left| D\rho\left(\frac{x-y}{\varepsilon}\right) \right| |g_k(y)| dy \\ &\leq \varepsilon^{-(n+1)} \sup_{z \leq 1} \rho(z) \int_{\mathbb{R}^n} |g_k(y)| dy \\ &\leq \frac{C_0}{\varepsilon^{n+1}} \sup_{|z| \leq 1} \rho(z). \end{aligned}$$

We can now apply the Arzelà-Ascoli theorem as follows: For each $\varepsilon > 0$ we have a subsequence $\{g_{k_l,\varepsilon}\}_{l=0}^{\infty}$ of the sequence $\{g_{k,\varepsilon}\}_{k=0}^{\infty}$ converging uniformly on the set $\overline{\Omega}$. We now set $\varepsilon_m = \frac{1}{m}$ with $m = 1, 2, ...,$ and with the aid of Cantor's diagonalisation procedure we select a subsequence $\{g_{k_l}\}_{l=0}^{\infty}$ of the sequence $\{g_k\}_{k=0}^{\infty}$ with the following property: For each fixed $m \in \mathbb{N}$ the sequence $\{g_{k_l,\varepsilon_m}\}_{l=0}^{\infty}$ converges uniformly in the set $\overline{\Omega}$.

The inequality

$$|g_k(x) - g_{k,\varepsilon}(x)| \leq \int_{|z| \leq 1} \rho(z) |g_k(x) - g_k(x - \varepsilon z)| dz \quad \leq \int_{|z| \leq 1} \rho(z) \int_0^{\varepsilon} |Dg_k(x - tz|) dt dz$$

holds for all $x \in \Omega$ which implies the estimate

$$\int_{\Omega} |g_k(x) - g_{k,\varepsilon}(x)| dx \leq \varepsilon \int_{\Omega} |Dg_k(x)| dx \leq C_1 \varepsilon$$

for all $k \in \mathbb{N}$. We can choose an arbitrary ε and obtain

$$\begin{aligned}\|g_{k_{l_1}} - g_{k_{l_2}}\|_1 &\leq \|g_{k_{l_1}} - g_{k_{l_1,\varepsilon_m}}\|_1 + \|g_{k_{l_1,\varepsilon_m}} - g_{k_{l_2,\varepsilon_m}}\|_1 + \|g_{k_{l_2,\varepsilon_m}} - g_{k_{l_2}}\|_1 \\ &= (2C_1 + |\Omega|)\varepsilon \quad \text{for all } l_1, l_2 \geq l_0(\varepsilon).\end{aligned}$$

We determine m sufficiently large and afterwards choose $l_1, l_2 \geq l_0(\varepsilon, m(\varepsilon)) =: l_0(\varepsilon)$. Consequently, $\{g_{k_l}\}_{l=1}^{\infty}$ is a Cauchy sequence in $L^1(\Omega)$ and thus converges since $L^1(\Omega)$ is a Banach space.

We therefore know that the adjoint sequence $\{f_{k_l}\}_{l=1}^{\infty}$ also converges in $L^1(\Omega)$ by the inequality

$$\|g_k - f_k\|_1 \leq c\|g_k - f_k\|_{1,p,\Omega} \leq \frac{c}{k}.$$

We can extend this to the cases $q < \frac{np}{n-p}$ by estimating

$$\begin{aligned}\|f\|_q &\leq \|f\|_1^{\lambda}\|f\|_{\frac{np}{n-p}}^{1-\lambda} \quad \text{where } \lambda + (1-\lambda)\left(\frac{1}{p} - \frac{1}{n}\right) = q \text{ by (7)} \\ &\leq \|f\|_1^{\lambda}(C\|Df\|_p)^{1-\lambda} \quad \text{by (2)}.\end{aligned}$$

We therefore have the result of the theorem that a bounded set in $W_0^{1,p}(\Omega)$ must be precompact in $L^q(\Omega)$ when $q < \frac{np}{n-p}$ for $p < n$. □

3.4 Corollary

The Rellich-Kondrachov compactness theorem now allows us to extend the statement of the Sobolev embedding theorem. Since we have that $W_0^{1,p}(\Omega)$ is compactly embedded in the spaces $L^q(\Omega)$ for any $1 \leq q < \frac{np}{n-p}$ where $p < n$, it must also be the case that $W_0^{1,p}(\Omega) \hookrightarrow L^q(\Omega)$ for any $1 \leq q < \frac{np}{n-p}$ and $p < n$ since a compact embedding implies a continuous embedding.

4 Consequences of Sobolev Embedding and Rellich-Kondrachov Compactness: $C_p(\Omega)$ is achieved by a positive Function u_p^*

In particular, we can use the above two theorems to deduce the following result: Let

$$S_p(\Omega) = \sup\left\{ \frac{(\int_\Omega |u(x)|^p dx)^{\frac{1}{p}}}{(\int_\Omega |\nabla u(x)|^2 dx)^{\frac{1}{2}}} \middle| u \in W_0^{1,2}, u \not\equiv 0 \right\} \quad 1 \leq p < \frac{2n}{n-2}.$$

Then it is clear that $S_p(\Omega)$ gives the sharp constant for the Sobolev embedding $W_0^{1,2}(\Omega) \hookrightarrow L^p(\Omega)$. We therefore have that $S_p(\Omega)$ is finite.

To show that this supremum is achieved, we take a sequence of functions $\{u_j\} \in W_0^{1,2}(\Omega)$ with the properties that $\|u\|_{1,2,\Omega} = \|\nabla u\|_2 = 1$ (which we can do without loss of generatily since the quotient we are minimising is scale invariant) and $\frac{\|u\|_p}{\|\nabla u\|_2} \to S_p(\Omega)$. By Rellich-Kondrachov Compactness there exists a subsequence $\{u_{j_k}\}$ which converges to a limit function $u^* \in L^p(\Omega)$. By uniqueness of limits, it must be the case that $\frac{\|u^*\|_p}{\|\nabla u^*\|_2} = S_p(\Omega)$.

As given by Gilbarg and Trudinger ([6] section 7.4), we note that for $u \in W^1(\Omega)$ we have that $|u| \in W^1(\Omega)$

$$\nabla|u| = \begin{cases} \nabla u & \text{if } u > 0 \\ 0 & \text{if } u = 0 \\ -\nabla u & \text{if } u < 0. \end{cases}$$

Setting $v^* = |u^*|$ we therefore have that

$$\|Dv^*\|_2 = \left(\int_\Omega |\nabla v^*(x)|^2 dx\right)^{\frac{1}{2}} = \left(\int_\Omega |\nabla |u^*(x)||^2 dx\right)^{\frac{1}{2}} = \left(\int_\Omega |\nabla u^*(x)|^2 dx\right)^{\frac{1}{2}} = \|Du^*\|_2.$$

It is also clear that $\|v^*\|_p = \|u^*\|_p$. It is for this reason that we can choose $u^* \geq 0$.

Equivalently, for

$$C_p(\Omega) = \frac{1}{(S_p(\Omega))^2} = \inf\left\{\phi_p(u) = \frac{\int_\Omega |\nabla u(x)|^2 dx}{(\int_\Omega |u(x)|^p dx)^{\frac{2}{p}}}\middle| u \in W_0^{1,2}, u \geq 0, u \not\equiv 0\right\} \quad 1 \leq p < \frac{2n}{n-2}$$

we have that $C_p(\Omega)$ is finite and that it is realised by a positive function u_p^*.

We can therefore look to solve for u_p^* and $C_p(\Omega)$ on domains with $n \geq 3$ and $1 \leq p < \frac{2n}{n-2}$, while we note that on domains in the plane there is no restriction on p besides $p \geq 1$ (see [2]).

5 Properties of u_p^*

5.1 u_p^* as a Solution to the Euler-Lagrange equation

The derivation of the Euler-Lagrange equation is based on the derivation in [2]. Noting that $\phi_p(u)$ is scale invariant, i.e. $\phi_p(ku) = \phi_p(u)$, we can reformulate the condition that u_p^* is a minimum of $\phi_p(u)$ as a constrained minimum problem

$$\min \phi_p(u) \quad \text{subject to} \quad \int_\Omega u(x)^p dx = 1.$$

Set

$$\mathcal{L} = \int_\Omega |\nabla u(x)|^2 dx + \lambda\left(1 - \int_\Omega u(x)^p dx\right).$$

Setting the Frèchet derivative of $\mathcal{L}$ equal to zero then gives

$$\frac{d}{d\varepsilon}\bigg|_{\varepsilon=0} \int_\Omega |\nabla(u(x) + \varepsilon v(x))|^2 d\mu = \frac{d}{d\varepsilon}\bigg|_{\varepsilon=0} \Lambda \int_\Omega (u(x) + \varepsilon v(x))^p dx.$$

Density of $C_0^\infty(\Omega)$ in both $L^p(\Omega)$ and $W_0^{1,2}$ allows us to take $u, v \in C_0^\infty(\Omega)$ without loss of generality and thus we can differentiate under the integral sign

$$\int_\Omega 2\nabla u(x) \cdot \nabla v(x) dx = \lambda \int_\Omega p u(x)^{p-1} v dx.$$

Letting $\Lambda = \frac{\lambda p}{2}$, we have

$$\int_\Omega \big(- \nabla u(x) \cdot \nabla v(x) - \Lambda u(x)^{p-1} v\big) dx = \int_\Omega v(x)\big(\Delta u(x) - \Lambda u(x)^{p-1}\big) dx = 0,$$

and since $v \in C_0^\infty(\Omega)$ is arbitrary, it must be the case that u solves the Euler-Lagrange equation

$$\Delta u - \Lambda u^{p-1} = 0 \quad \text{with } u\big|_{\partial\Omega} = 0 \tag{9}$$

for some constant Λ.

This is a generalised eigenvalue problem of the Laplacian. However, for our purposes it will not be necessary to find the eigenvalues and it will often simplify our approach to set $\Lambda = 1$.

5.2 Symmetry of positive Solutions u_p^*

Gidas, Ni and Nirenberg [5] have shown that u_p^* possesses symmetry properties which will prove to be very useful in our effort to find solutions.

They present the following theorem:

Theorem 5.2.1. *On the ball $B_R(0)$ of radius R in $\mathbb{R}^n$, let $u > 0$ be a positive solution in $C^2(\overline{\Omega})$ of*

$$\Delta u + f(u) = 0 \quad \textit{subject to } u|_{\partial B_R(0)} = 0,$$

where $f \in C^1$. Then u is radially symmetric and

$$\frac{\partial u}{\partial r} < 0, \ \textit{for } 0 < r < R.$$

Generalisations to other domains are also presented in the paper, with the important idea for us that the solution inherits any symmetry properties that the domain possesses.

6 Introduction of Methods for finding u_p^*

There is a fair amount of literature devoted to finding solutions to problems of the type

$$\Delta u + f(u) = 0 \quad \text{subject to} \quad u\big|_{\partial\Omega} = 0.$$

The most successful numerical schemes make use of the fact that solutions of this equation correspond to critical points of the energy functional

$$I(u) = \int_\Omega (\frac{1}{2}|\nabla u(x)|^2 - F(u(x)))dx, \tag{10}$$

where $F(u) = \int_0^u f(t)dt$.

A fundamental paper in this field by Ambrosetti and Rabinowitz [1] guarantees the existence of critical points of a functional like $I(u)$ which lie on a path between a local minimum (in our case the zero solution, which we want to avoid) and a point of lower altitude, subject to certain conditions. These critical points can be visualised as saddle points on a mountain pass between the local minimum and the point of lower altitude, leading to the name "Mountain Pass Theorem".

It can help to imagine a valley surrounded on all sides by a ridge with a long (in our case infinite) descent outside of the ridge in each direction, much like the top of a volcano. Altitude here is determined by the functional value. The rim of the volcano is not of uniform height and so the lowest points on the rim are saddle points. It is precisely these points which we are trying to find.

A projection onto the point of highest altitude (the rim of the volcano) on the linear path between any function and the zero solution, mapping out a subset of $W_0^{1,2}$ called the Nehari Manifold, is highly useful in finding these saddle points in conjunction with the method of steepest descents.

Essentially, the algorithm employed finds a point on the Nehari manifold and then travels along the manifold in the descent direction to find a minimum point on the manifold that corresponds to a saddle point solution.

The key results which lead to the algorithm that was employed will now be presented.

7 Key Ingredients to designing the Solution Algorithm

7.1 Mountain Pass Theorem

A fundamental paper in this field is by Ambrosetti and Rabinowitz [1] in which the authors present a result known as the "Mountain Pass Theorem". The following definition will be relevant:

Palais-Smale Condition

A continuously Fréchet differentiable functional $I \in C^1(H, \mathbb{R})$ from a Hilbert space H to the real numbers satisfies the Palais-Smale condition if every sequence $\{u_k\}_{k=0}^{\infty} \subset H$ satisfying

- $\{I[u_k]\}_{k=0}^{\infty}$ is bounded, and
- $I'[u_k] \to 0$ in H

has a convergent subsequence in H.

The statement of the theorem (see [1]) is as follows:

Theorem 7.1.1. *Let E be a real Banach space and $I \in C^1(E, \mathbb{R})$, satisfying the Palais-Smale condition. Suppose that there are two points u_0 and $u_1 \in E$ and constants ρ and α such that the following conditions hold true:*

- *$I(u) \geq \alpha$ for all $u \in \partial B_\rho(u_0) = \{u \in E : \|u - u_0\| = \rho\}$;*
- *$\|u_0 - u_1\| > \rho$;*
- *$I(u_0)$ and $I(u_1) < \alpha$.*

Then I possesses a critical point $\overline{u} \neq 0$, $\overline{u} \neq u_0, u_1$, such that $f(\overline{u}) = c \geq a$. Moreover, c can be characterized as

$$c = c(\Gamma, I) = \inf_{\gamma \in \Gamma}[\max\{I(\gamma(t)) : 0 \leq t \leq 1\}]$$

where

$$\Gamma = \{\gamma \in C([0,1], E) : \gamma(0) = u_0 \text{ and } \gamma(1) = u_1\}.$$

7.2 Nehari Solution Manifold

Z Nehari [8] introduced the idea of defining a solution submanifold on which a local minimizer of the energy functional provides the desired solutions. Ni [9] showed that a global minimizer of the energy functional on the solution submanifold $\mathcal{M}$ defined by

$$\mathcal{M} = \left\{ u \in W_0^{1,2} : u \not\equiv 0, \int_\Omega [|\nabla u(x)|^2 - u(x) f(u(x))] dx = 0 \right\}$$

is a solution to our differential equation, under the condition that $f'(t) > \frac{f(t)}{t}, t \neq 0$. For $f(u) = u^{p-1}$ this means that $p > 2$. This restriction will have important consequences for the valid range for p in our nonlinear algorithm, namely that it likely will not work for $p < 2$.

Li and Zhou [7] describe a projection onto this solution manifold which for our problem takes the form

$$P_{\mathcal{M}} : W_0^{1,2} \backslash \{0\} \to \mathcal{M} : u \mapsto \left(\frac{\int_\Omega |\nabla u(x)|^2 dx}{\int_\Omega u(x)^p dx} \right)^{\frac{1}{p-2}} u. \tag{11}$$

By our earlier analogy, the Nehari manifold is the rim of the volcano on which we are trying to find the minima.

8 Numerical Procedures in the literature

8.1 Choi-McKenna Algorithm

Choi and McKenna [3] published a fundamental paper in applying the ideas of the Mountain Pass Theorem to a numerical algorithm.

Their idea was to take a linear path between between a local minimum u_0 (e.g. the zero solution) and a function of lower altitude u_1 and to deform this path by pushing the point of highest altitude on the path in the direction of steepest descent until a saddle point is found.

8.2 Li-Zhou Algorithm

Li and Zhou [7] improved this idea by using the projection (11) to map an initial guess onto the Nehari manifold. Their algorithm then travels in the direction of steepest descent, but makes sure to return to the Nehari manifold at each step via another projection. They only claim that their algorithm will be successful in the case $p > 2$.

This method thus cleverly avoids a problem in the Choi-McKenna algorithm where it is possible to keep straying further from the desired solution by following the steepest descent direction. In addition to this, it is computationally much more efficient since it avoids having to evaluate the functional for all of the points on the connecting path.

9 Application of the Li-Zhou Algorithm

We will be able to apply the above results and methods to find solutions to our problem

$$\Delta u + \Lambda u^{p-1} = 0 \quad \text{where } 1 \leq p < \frac{2n}{n-2} \quad \text{s.t.} \quad u\big|_{\partial\Omega} = 0; u \geq 0; u \not\equiv 0.$$

Different approaches will be appropriate for different values of p.

9.1 Superlinear Case: $p > 2$

Here we will set $\Lambda = 1$ for convenience.

Firstly we note that by Rellich's Theorem, the Palais-Smale compactness condition is met for the energy functional of this equation $I(u) = \int_\Omega (\frac{1}{2}|\nabla u(x)|^2 - \frac{u(x)^p}{p})dx$ for $1 \leq p < \frac{2n}{n-2}$, which includes the range for p in which we are interested.

Choi and McKenna [3] note that the energy functional $I(u) = \int_\Omega (\frac{1}{2}|\nabla u(x)|^2 - \frac{u(x)^p}{p})dx$ has a local minimum of 0 at the solution $u \equiv 0$. Moreover, when we take any positive function $v \in W_0^{1,2}$ and scale it by a constant c, we have that $I(cv) \to -\infty$ as $c \to \infty$ because the negative term dominates for large u. By the mountain pass theorem, we can thus conclude the existence of a separate solution u^* with the property that $I(u^*) > 0$.

We can further use the fact that $p > 2$ to conclude that a critical point of $I(u)$ will be found on the Nehari manifold

$$\mathcal{M} = \left\{ u \in W_0^{1,2} : u \not\equiv 0, \int_\Omega [|\nabla u(x)|^2 - u(x)^p]dx = 0 \right\}$$

which we can reach from any function u via the projection

$$P_{\mathcal{M}} : W_0^{1,2} \backslash \{0\} \to \mathcal{M} : u \mapsto \left(\frac{\int_\Omega |\nabla u(x)|^2 dx}{\int_\Omega u(x)^p dx} \right)^{\frac{1}{p-2}} u.$$

Our numerical algorithm will further require computation of the steepest descents direction. Choi and McKenna [3] argue that the steepest descent direction of $I(u)$ at $u \in W_0^{1,2}(\Omega)$ is given

by the function $v \in W_0^{1,2}(\Omega)$ with $\|v\|_{1,2,\Omega}$ such that the Fréchet derivative of $I(u)$ at u on v has a negative local minimum. The Fréchet derivative of $I(u)$ at u on v is

$$\begin{aligned}\left.\frac{d}{d\varepsilon}\right|_{\varepsilon=0} I(u+\varepsilon v) &= \left.\frac{d}{d\varepsilon}\right|_{\varepsilon=0} \int_\Omega \left(\frac{1}{2}|\nabla(u(x)+\varepsilon v(x))|^2 - \frac{(u(x)+\varepsilon v(x))^p}{p}\right)dx \\ &= \int_\Omega \big(\nabla u(x)\cdot\nabla v(x) - u(x)^{p-1}v(x)\big)dx.\end{aligned}$$

We therefore turn the problem into an unconstrained minimisation of

$$\mathcal{L} = \int_\Omega \big(\nabla u(x)\cdot\nabla v(x) - u(x)^{p-1}v(x)\big)dx + \lambda\Big(\int_\Omega |\nabla v(x)|^2 dx - 1\Big)$$

Setting the Fréchet derivative of $\mathcal{L}$ equal to zero gives

$$\int_\Omega \big(\nabla u(x)\cdot\nabla w(x) - u(x)^{p-1}w(x) + 2\lambda\nabla v(x)\cdot\nabla w(x)\big)dx = 0.$$

This means that the steepest descent direction $v \in W_0^{1,2}$ corresponds to a weak solution of

$$2\lambda\Delta v = -\Delta u - u^{p-1}, \tag{12}$$

where the right hand side will be non-zero if u is not a solution to (1). This process amounts to a linearisation since we now solve an equation for v that is linear is v. λ is calculated such that $\|v\|_{1,2,\Omega} = 1$, while to find the sign of λ we consider the approximation to the Fréchet derivative of the energy functional

$$\begin{aligned}\frac{I(u+\varepsilon v) - I(u)}{\varepsilon} &= \int_\Omega [\nabla u(x)\cdot\nabla v(x) - u(x)^{p-1}v(x)]dx + \mathcal{O}(\varepsilon) \\ &= \int_\Omega -2\lambda\nabla v(x)\cdot\nabla v(x)dx + \mathcal{O}(\varepsilon) \\ &= -2\lambda + \mathcal{O}(\varepsilon) \quad \text{since } \|v\|_{1,2,\Omega} = 1.\end{aligned}$$

The left term dominates as $\varepsilon \to 0$ so we choose λ positive to ensure that v represents the descent direction.

Choi and McKenna [3] argue that their algorithm preserves any symmetry obtained from an initial guess, and our addition of the Nehari projection which is merely a multiplication by a constant, will thus also preserve such symmetry. By the generalisations of Theorem (5.2.1) presented in [5] we know that u_p^* will possess the symmetry properties of the domain, and we will thus choose as our initial guess a function that has the expected symmetry properties.

9.1.1 Finite Element Approximation to the Steepest Descent Direction v

We will approximate the steepest descent direction via finite elements, taking u as known at the mesh points (by an initial guess or by the result of a previous iteration). Writing $\overline{v} = 2\lambda v + u$, the solution to (12) is given by the solution to

$$\Delta\overline{v} = -u^{p-1} \tag{13}$$

from which we can recover the steepest descent direction v.

To solve for $\overline{v} \in W_0^{1,2}(\Omega)$ we will solve the weak form of (13) with $w \in W_0^{1,2}(\Omega)$ representing the test function

$$\int_\Omega \nabla w(x)\cdot\nabla\overline{v}(x)dx = \int_\Omega w(x)u(x)^{p-1}dx. \tag{14}$$

We will now derive the finite element formulation based on the methods presented by Fish and Belytschko [4]. We firstly notice that we can split up our integral as a sum of the integrals over the individual element domains Ω^e:

$$\sum_{e=1}^{n_{el}} \left\{ \int_{\Omega^e} \nabla w^e(x) \nabla \overline{v}^e(x) dx - \int_{\Omega^e} w^e(x) (\overline{v}^e(x))^{p-1} dx \right\} = 0.$$

Now we now write our functions w and $\overline{v}$ in terms of their finite element approximations as:

$$w(x) \approx w^h(x) = \boldsymbol{N}(x)\boldsymbol{w}, \qquad \overline{v}(x) \approx \overline{v}^h(x) = \boldsymbol{N}(x)\boldsymbol{d},$$

where $\boldsymbol{N}$ are shape functions with value 1 at their corresponding mesh point and value 0 at all other mesh points, while $\boldsymbol{w}$, $\boldsymbol{d}$ are vectors of nodal function values. The gradients of w and $\overline{v}$ can then be written as

$$\nabla w \approx \boldsymbol{B}(x)\boldsymbol{w}, \qquad \nabla \overline{v} \approx \boldsymbol{B}(x)\boldsymbol{d},$$

where $\boldsymbol{B}$ are the gradients of the shape functions. We can rewrite the above expressions for the element level as

$$w^e(x) \approx \boldsymbol{N}^e(x)\boldsymbol{w}^e, \quad \overline{v}^e(x) \approx \boldsymbol{N}^e(x)\boldsymbol{d}^e, \quad \nabla w^e \approx \boldsymbol{B}^e(x)\boldsymbol{w}^e, \quad \nabla \overline{v}^e \approx \boldsymbol{B}^e(x)\boldsymbol{d}^e.$$

Rewriting the integral using these approximations leaves us with

$$\sum_{e=1}^{n_{el}} \left\{ \int_{\Omega^e} \boldsymbol{w}^{e^T} \boldsymbol{B}^{e^T}(x) \boldsymbol{B}^e(x) \boldsymbol{T}^e dx - \int_{\Omega^e} \boldsymbol{w}^{e^T} \boldsymbol{N}^{e^T}(x) (\boldsymbol{N}^e(x)\boldsymbol{d}^e)^{p-1} dx \right\} = 0,$$

since $\boldsymbol{B}^e(x)\boldsymbol{w}^{eT} = \boldsymbol{w}^{e^T}\boldsymbol{B}^{e^T}(x)$ and $\boldsymbol{N}^e(x)\boldsymbol{w}^{eT} = \boldsymbol{w}^{e^T}\boldsymbol{N}^{e^T}(x)$. We notice that we can take the constants $\boldsymbol{w}^{e^T}$ and $\boldsymbol{d}^e$ outside of the integral to give

$$\sum_{e=1}^{n_{el}} \boldsymbol{w}^{e^T} \left\{ \int_{\Omega^e} \boldsymbol{B}^{e^T}(x) \boldsymbol{B}^e(x) dx \boldsymbol{d}^e - \int_{\Omega^e} \boldsymbol{N}^{e^T}(x) (\boldsymbol{N}^e(x)\boldsymbol{d}^e)^{p-1} dx \right\} = 0.$$

Letting

$$\boldsymbol{K}^e = \int_{\Omega^e} \boldsymbol{B}^{e^T}(x) \boldsymbol{B}^e(x) dx \quad \text{and} \quad \boldsymbol{f}^e = \int_{\Omega^e} \boldsymbol{N}^{e^T}(x) (\boldsymbol{N}^e(x)\boldsymbol{d}^e)^{p-1} dx$$

and using the gather matrix to write

$$\boldsymbol{w}^e = \boldsymbol{L}^e\boldsymbol{w}, \quad \boldsymbol{d}^e = \boldsymbol{L}^e\boldsymbol{d},$$

we get

$$\boldsymbol{w}^T \left(\sum_{e=1}^{n_{el}} \boldsymbol{L}^{e^T} \boldsymbol{K}^e \boldsymbol{L}^e \boldsymbol{d} - \sum_{e=1}^{n_{el}} \boldsymbol{L}^{e^T} \boldsymbol{f}^e \right) = 0.$$

Further letting

$$K = \sum_{e=1}^{n_{el}} \boldsymbol{L}^{e^T} \boldsymbol{K}^e \boldsymbol{L}^e \boldsymbol{d} \quad \text{and } \boldsymbol{f} = \sum_{e=1}^{n_{el}} \boldsymbol{L}^{e^T} \boldsymbol{f}^e = 0,$$

we end up with

$$\boldsymbol{w}^T(\boldsymbol{K}\boldsymbol{d} - \boldsymbol{f}) = 0 \quad \forall \boldsymbol{w}.$$

Since we know that $w \in W_0^{1,2}$ is arbitrary we therefore solve the discrete finite element form

$$\boldsymbol{K}\boldsymbol{d} = \boldsymbol{f}, \tag{15}$$

with $\boldsymbol{N}\boldsymbol{d}$ the finite element approximation to $\overline{v}$ from which we can recover the steepest descent direction v.

9.1.2 Solution Algorithm for $p > 2$

Step 1:

We start with an initial guess $u = u_{guess}$ that maintains the symmetries of the domain Ω.

Step 2:

We apply the Nehari projection (11), setting $u \leftarrow P_{\mathcal{M}}(u)$.

Step 3:

We compute the steepest descent direction v and set $g \leftarrow v$.

Step 4:

If $\|g\|_{1,2,\Omega} \leq$ Tolerance, we are done. Otherwise, apply the Nehari projection, setting $u_{next} \leftarrow P_{\mathcal{M}}(u + g)$.

Step 5:

If $I(u_{next}) < I(u)$, set $u \leftarrow u_{next}$ and go to step 3. Otherwise set $g \leftarrow \frac{g}{2}$ and go to step 4.

The final value u represents an approximation to our desired solution u^*.

9.2 Sublinear Case: $p < 2$

For the sublinear case $p < 2$ we can use the negative energy functional

$$I_{neg}(u) = -I(u) = \int_\Omega \left(\frac{u(x)^p}{p} - \frac{1}{2}|\nabla u(x)|^2 \right) dx \tag{16}$$

The Palais-Smale condition is again satisfied for $1 \leq p < \frac{2n}{n-2}$, which includes the range for p in which we are interested.

We again note that the functional $I_{neg}(u) = \int_\Omega (\frac{1}{2}|\nabla u(x)|^2 - \frac{u(x)^p}{p})dx$ has a local minimum of 0 at the solution $u \equiv 0$. Moreover, when we take any positive function $v \in W_0^{1,2}$ and scale it by a constant c, we have that $I(cv) \to -\infty$ as $c \to \infty$ because the negative term dominates for large u. By the mountain pass theorem, we can thus conclude the existence of a separate solution u^* with the property that $I(u^*) > 0$.

In this case, however, we cannot conclude as in the case of $p > 2$ that the saddle point solution will be found on the Nehari manifold.

Nevertheless, we apply the algorithm (with obvious sign adjustments as a result of the sign change in the functional $I_{neg}(u)$) in the hope that it will work in spite of this. As discussed in the sections on numerical verification of the results, a numerical test of the functions given by the algorithm seems to indicate that the algorithm fails in this case. The results are nevertheless included for completeness.

In particular, these sign changes mean that we now define $\overline{v} = 2\lambda v - u$ and solve $\Delta \overline{v} = u^{p-1}$ or equivalently, in weak form

$$\int_\Omega \nabla w(x) \cdot \nabla \overline{v}(x) dx = -\int_\Omega w(x) u(x)^{p-1} dx. \tag{17}$$

In finite element form, our approximation to $\overline{v}$ is given by $\boldsymbol{N}\boldsymbol{d}$ where $\boldsymbol{d}$ is the solution to $\boldsymbol{K}\boldsymbol{d} = -\boldsymbol{f}$ with $\boldsymbol{K}$, $\boldsymbol{N}$ and $\boldsymbol{f}$ defined as in (7). The only change in our algorithm is in using $I_{neg}(u)$ in place of $I(u)$ and making the changes discussed above when calculating the steepest descent direction v.

9.3 Linear Cases $p = 1$ and $p = 2$

For $p = 1$ and $p = 2$ the problem becomes linear and is thus simpler to solve.

For $p = 1$ we solve the equation

$$\Delta u + \Lambda = 0 \quad \text{s.t.} \quad u\big|_{\partial\Omega} = 0; u \geq 0; u \not\equiv 0, \tag{18}$$

which in weak form immediately yields a linear system of equations by finite element approximation which can be easily solved.

For $p = 2$ we solve the equation

$$\Delta u + \Lambda u = 0 \quad \text{s.t.} \quad u\big|_{\partial\Omega} = 0; u \geq 0; u \not\equiv 0, \tag{19}$$

which in weak form yields a generalised eigenvalue problem by finite element approximation, easily solved.

10 Numerical Results

The algorithm was implemented to find solutions, distribution functions and the constant $C_p(\Omega)$ on the unit ball in n dimensions (results given for $n = 4$), on the unit square in the plane as well as on a rectangle in the plane.

Graphs are used to summarise the results along with plots of the solutions.

10.1 Unit Ball

The n-dimensional unit ball $B_1^n(0)$ centred at the origin is easy to treat due to the known radial symmetry of solutions to (1) (see Theorem (5.2.1)). This turns the n-dimensional problem into a 1 dimensional problem as follows:

If u is a radial function $u = u(r)$ then we can write

$$\Delta u + \Lambda u^{p-1} = 0 \quad \text{with } u\big|_{\partial\Omega} = 0, u \geq 0, u \not\equiv 0$$

as

$$r^{1-n}\frac{\partial}{\partial r}\left(r^{n-1}\frac{\partial u}{\partial r}\right) + \Lambda u^{p-1} = 0 \quad \text{with } u(1) = 0, \left.\frac{du}{dr}\right|_{r=0} = 0, u \geq 0, u \not\equiv 0 \tag{20}$$

by use of the radial Laplacian. The problem is thus turned into a one dimensional problem with the boundary condition reducing to $u(1) = 0$. In addition, since we are looking for smooth solutions, we can conclude that $\frac{du}{dr}|_{r=0} = 0$.

We further have that, for any radial function $v = v(r)$

$$\begin{aligned}
\int_{B_1^n(0)} v(x)dx &= \int_{S_1^{n-1}(0)} \int_0^1 v(r) r^{n-1} dr d\theta \\
&= \int_0^1 v(r) r^{n-1} dr \int_{S_1^{n-1}(0)} d\theta \\
&= \int_0^1 v(r) r^{n-1} dr \times \text{Area}(S_1^{n-1}(0)) \\
&= \int_0^1 v(r) r^{n-1} dr \times \frac{(n-1)\pi^{\frac{n-1}{2}}}{\Gamma(\frac{n-1}{2}+1)},
\end{aligned}$$

where $\int_{S_1^{n-1}(0)}$ is the sphere in n dimensions with $n-1$ dimensional measure. Lastly, if u solves (20) weakly and $w = w(r)$ is a radial test function then

$$\begin{aligned}
&\int_{B_1^n(0)} w(x)(\Delta u(x) + \Lambda u(x)^{p-1})dx = 0 \\
\Rightarrow &\int_{S_1^{n-1}(0)} \int_0^1 w(r)\left[r^{1-n}\frac{\partial}{\partial r}\left(r^{n-1}\frac{\partial u(r)}{\partial r}\right)u + \Lambda u(r)^{p-1}\right]r^{n-1}drd\theta = 0 \\
\Rightarrow &\int_0^1 \left[-r^{1-n}\frac{\partial w(r)}{\partial r}\left(r^{n-1}\frac{\partial u(r)}{\partial r}\right) + w\Lambda u(r)^{p-1}\right]r^{n-1}dr \int_{S_1^{n-1}(0)} d\theta = 0 \\
\Rightarrow &\int_0^1 \left[-r^{1-n}\frac{\partial w(r)}{\partial r}\left(r^{n-1}\frac{\partial u(r)}{\partial r}\right) + w(r)\Lambda u(r)^{p-1}\right]r^{n-1}dr = 0. \qquad (21)
\end{aligned}$$

This will be useful in verifying numerically whether our solutions solve the problem weakly.

According to the discussion in the sections above, the problem can now be solved by finite element analysis for $2 < p < \frac{2n}{n-2}$ using the Li-Zhou algorithm as well as for $p = 1, 2$ using standard linear methods. For the nonlinear cases, the initial guess is taken as the solution for $p = 1$, as this solution is found to possess the correct symmetry properties. Λ is set to 1 for simplicity.

The problem was solved for a number of dimensions along with a verification of the results in each case. We will present the results for the case of 4 dimensions.

Fig. 1 below shows the radial solution $u(r)$ for values of p chosen to provide a good idea of how the solutions behave over the permissible range for p. The solutions have been normalised so that $\sup(u) = 1$ so that they can be easily compared on the same axes.

Fig. 1: Radial Solution on the Unit Ball of Dimension 4

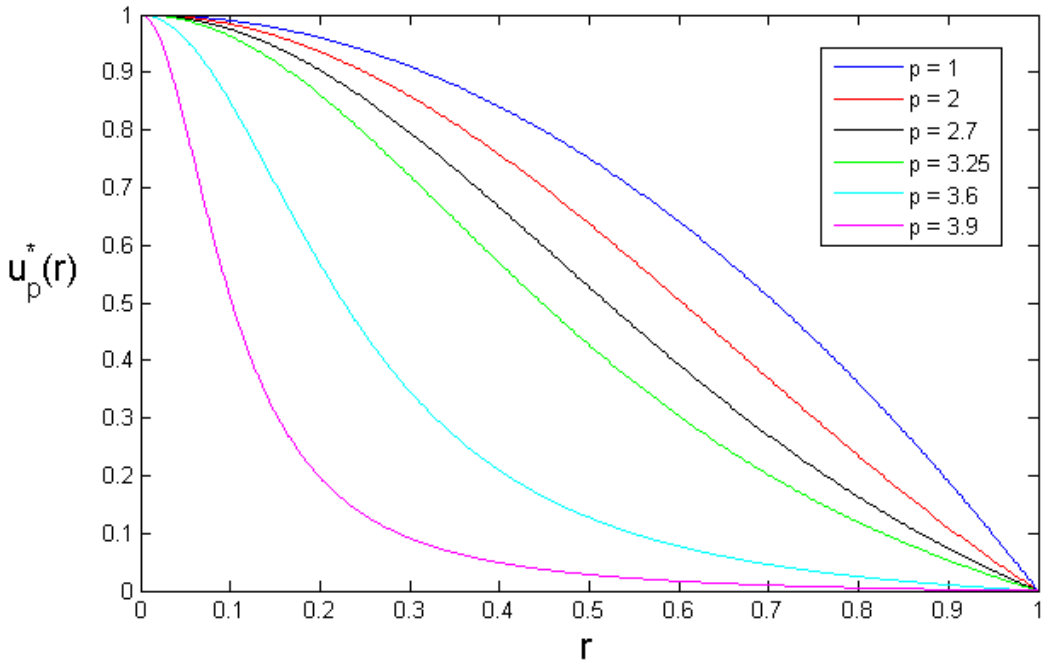

We see that the solutions have their maxima at the centre of the ball. It seems to be the case that the solution becomes more concentrated around the centre as the value of p grows. As p

tends toward the critical value of $\frac{2n}{n-2} = \frac{2\times 4}{4-2} = 4$, the solution seems to tend toward a function that has negligible value outside of a small range about the origin.

This can be formulated more precisely in terms of the distribution function

$$\mu_{p,\Omega}(t) = \text{Vol}(\{x \in \Omega | u(x) \geq t\}),$$

where it seems to be the case that $p < q \Rightarrow \mu_{p,\Omega}(t) \geq \mu_{q,\Omega}(t)$.

The distribution functions can be found by sampling the solution approximations at a large number of points. The number of points with function values above t is then divided by the total number of sampled points to approximate $\tilde{\mu}_{p,\Omega}(t) = \{r : u(r) \geq t\}$. Since $u(r)$ decreases monotonically (see Theorem (5.2.1)), we conclude that $\tilde{\mu}_{p,\Omega}(t) = \{r : 0 \leq r \leq r_t\}$ where $r_t = \{r : u(r) = t\}$. The volume $\mu_{p,\Omega}(t)$ is thus simply the volume of a ball with radius r_t and can be found as $\mu_{p,\Omega}(t) = \frac{\pi^{\frac{n}{2}}}{\Gamma(\frac{n}{2}+1)} r_t^n$.

The distribution functions are plotted in Fig. 2 below. We see that as p approaches 4, the distribution function seems to collapse toward a function negligible outside of a small neighbourhood of 0.

Fig. 2: Distribution Functions for Solutions on the Unit Ball of Dimension 4

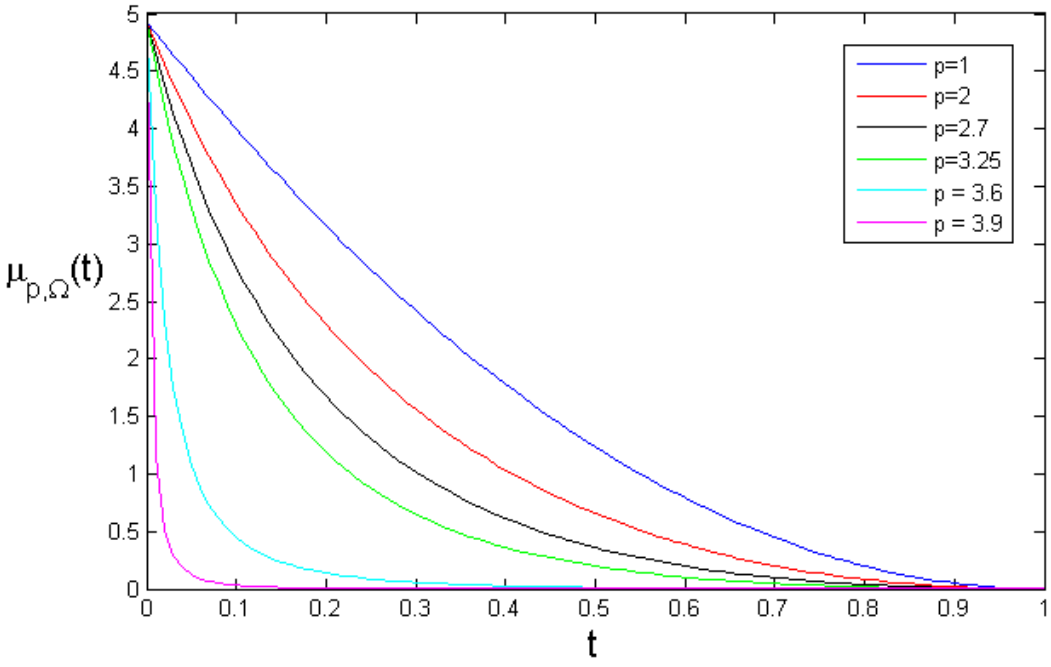

Thesis supervisor Dr Ratzkin had proposed a conjecture that the behaviour

$$p < q \Rightarrow \mu_{p,\Omega}(t) \geq \mu_{q,\Omega}(t) \quad \text{for all } t \in [0,1]$$

would be true for the distribution functions, and the above results give numerical evidence to support this hypothesis. Namely, according to our results summarised in Fig. 2, the distribution functions for higher p values lie below those with lower p values.

For values $1 < p < 2$ we have stated that there is no justification for the algorithm employed. Moreover, the functions that the algorithm converges on were shown to fail in solving the problem weakly (see section (10.2)). The distribution functions for some of these functions are plotted in Fig. 3 below and we see that the behaviour goes against the conjecture.

Fig. 3: Distribution Functions for Rejected Solutions on the Unit Ball of Dimension 4

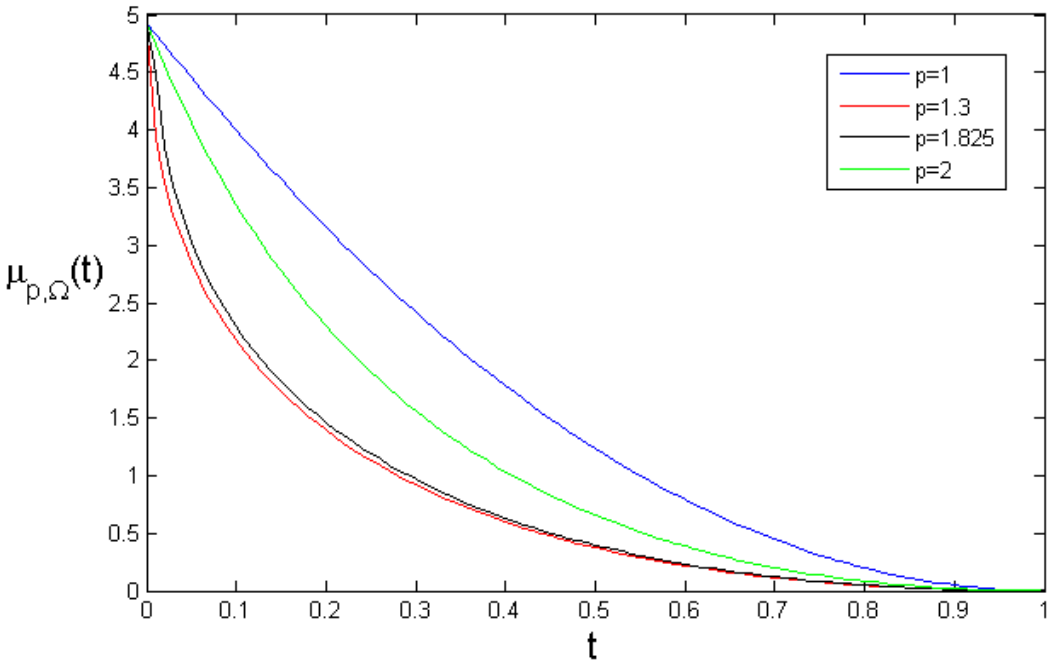

In fact many of the functions produced by the algorithm either have identical distribution functions to either the case $p = 1$, $p = 1.3$ or $p = 2$, which is why only a few distribution functions have been shown. It is clear that further investigation is required to find actual solutions in order to test the hypothesis for the cases $1 < p < 2$.

We now turn our attention to the behaviour of the sharp Sobolev constant $C_p(\Omega)$ on the unit ball as we vary p. In Fig. 4 below we see that the for $2 \leq p \leq 3.5$, $C_p(\Omega)$ decreases with p. $C_1(\Omega) < C_2(\Omega)$ while we see strange behaviour for $1 < p < 2$, attributable to the fact that the functions given by our algorithm are not actually solutions to (1).

Fig. 4: Behaviour of $C_p(\Omega)$ with varying p on the Unit Ball of Dimension 4

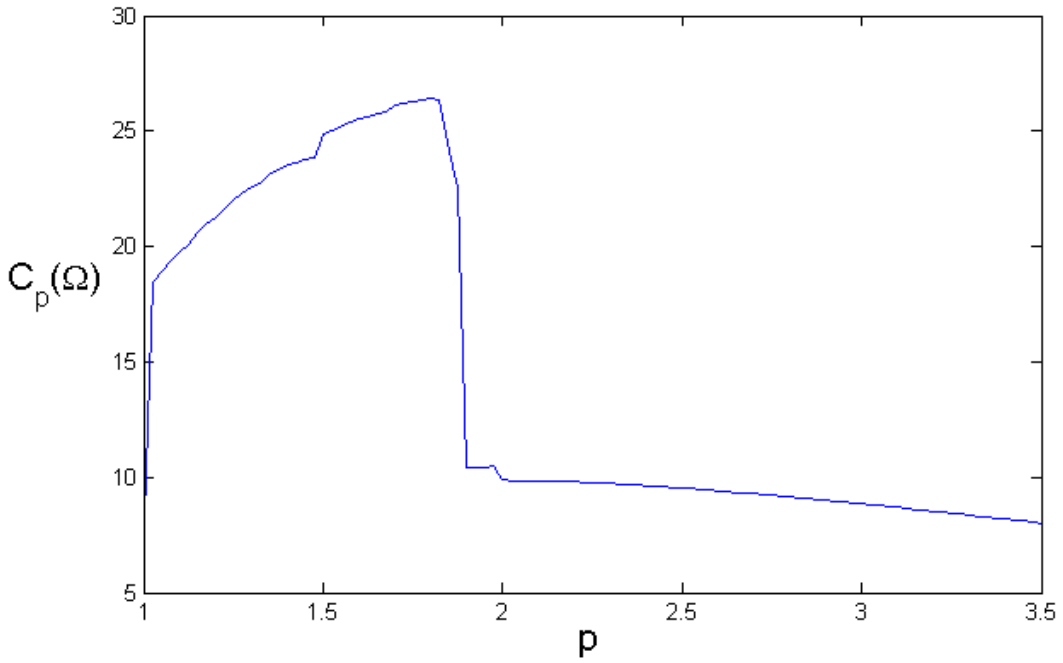

10.2 Verification of Results on Unit Ball

We will apply both analytical and numerical methods to verify our results. The problem (1) has known analytical solutions for the cases $p = 1$ and $p = 2$. For other values of p, we can test whether our supposed solutions solve the equation weakly using finite element approximation.

10.2.1 Analytical Solution for $p = 1$

The case of solving

$$r^{1-n}\frac{\partial}{\partial r}\left(r^{n-1}\frac{\partial u}{\partial r}\right) + \Lambda u^{p-1} = 0 \quad \text{subject to } u(1) = 0, \frac{du}{dr}|_{r=0} = 0$$

on the unit ball for $p = 1$ is straightforward. We can rewrite the above as

$$\Rightarrow \frac{d^2u}{dr^2} + \frac{n-1}{r}\frac{du}{dr} + \Lambda = 0.$$

We can now use the guess that u is a quadratic function $u(r) = ar^2 + br + c$ and apply the boundary conditions

$$\begin{aligned}\frac{du}{dr}|_{r=0} = 0 = 2a(0) + b = 0 \\ \Rightarrow b = 0\end{aligned}$$

and

$$\begin{aligned}u(1) = a + c = 0 \\ \Rightarrow a = -c.\end{aligned}$$

We then substitute $u(r) = ar^2 - a$ into the equation and obtain

$$2a + \frac{n-1}{r}2ar + \Lambda = 0$$
$$\Rightarrow a = -\frac{\Lambda}{2n}.$$

Our solution is thus $u(r) = -\frac{\Lambda}{2n}r^2 + \frac{\Lambda}{2n}$.

When the analytical solution is plotted over the result from our finite element implementation, the results are seen to be identical. This is expected since we have used quadratic shape functions on the elements and can thus perfectly replicate this quadratic solution.

10.2.2 Analytical Solution for $p = 2$

The case of solving

$$r^{1-n}\frac{\partial}{\partial r}\left(r^{n-1}\frac{\partial u}{\partial r}\right) + \Lambda u^{p-1} = 0 \quad \text{subject to } u(1) = 0, \frac{du}{dr}|_{r=0} = 0$$

for $p = 2$ is only slightly more difficult than for $p = 1$. We can write the problem as

$$\Rightarrow \frac{d^2u}{dr^2} + \frac{n-1}{r}\frac{du}{dr} + \Lambda u = 0. \tag{22}$$

We use the suggestion of Ratzkin [10] by looking for a solution of the form

$$f(r) = r^q J_a(kr), \tag{23}$$

where J_a is the Bessel function of weight a, and k and q are positive constants.
We start by substituting (23) into equation (22) and proceed to multiply equation by r^2, resulting in

$$\begin{aligned} 0 =& r^2[q(q-1)r^{q-2}J_a(kr) + 2qr^{q-1}J_a^{'}(kr)k + r^q J_a^{''}(kr)k^2] \\ &+ (n-1)r[qr^{q-1}J_a(kr) + r^q J_a^{'}(kr)k] + r^{q+2}\Lambda J_a(kr). \end{aligned}$$

Some regrouping leads to

$$0 = r^q\Big[J_a(kr)[q(q-1) + (n-1)q + \Lambda r^2] + J_a^{'}[rk(2q+n-2)] + rkJ_a^{'}(kr) + k^2r^2J_a^{''}(kr)\Big],$$

allowing us to replace the last two terms in the large parentheses by $(a^2 - k^2r^2)J_a(kr)$ using the defnition of the Bessel function according to the Bessel differential equation. We now have that

$$0 = r^q\Big[(2q+n-2)rkJ_a^{'}(kr) + (\Lambda - k^2)r^2J_a(kr) + [q(q-1) + (n-1)q + a^2]J_a(kr)\Big].$$

Noting that $rkJ_a^{'}$, r^2J_a and J_a are linearly independent, we can set their coefficients to zero and recover

$$q = \frac{2-n}{2} \quad k = \sqrt{\Lambda} \quad a = \frac{n-2}{2}.$$

Using the boundary condition $u(1) = 0$ gives $J_{\frac{n-2}{2}}(\sqrt{\Lambda}) = 0$, which means that $\sqrt{\Lambda}$ is in fact the first positive zero $j_{\frac{n-2}{2}}$ of $J_{\frac{n-2}{2}}$, since our solution $u(r) \geq 0$. We then have the solution

$$u(r) = r^{\frac{2-n}{2}}J_{\frac{n-2}{2}}(j_{\frac{n-2}{2}}r).$$

The solutions obtained via our finite element approximation for $p = 2$ correspond arbitrarily closely to this analytical solution, depending on how fine the element mesh is chosen. A plot of the analytical over the numerical solution leaves the two functions almost indistinguishable even for very few elements.

10.2.3 Numerical Verification of Results on the Unit Ball

As noted above (see (21)), any solution to (20) will satisy

$$WT_w(u) := \int_0^1 \left[- r^{1-n} \frac{\partial w(r)}{\partial r} \left(r^{n-1} \frac{\partial u(r)}{\partial r} \right) + w(r) \Lambda u(r)^{p-1} \right] r^{n-1} dr = 0 \tag{24}$$

The above lends itself well to testing via finite element approximation. A random test function $w(r)$ is created by randomly generating numbers at the mesh points and $WT_w(u)$ is evaluated by Gauss quadrature. For comparison purposes, the functions u are normalised so that $\sup(u) = 1$. This requires that Λ be rescaled (Λ is set equal to 1 in the algorithm for simplicity), and the appropriate rescaling is then given by a^{2-p} where a is the factor normalising u. This rescaling is derived from the fact that if u solves

$$\Delta u + u^{p-1} = 0 \tag{25}$$

then au solves

$$\Delta(au) + a^{2-p}(au)^{p-1} = 0,$$

by simply multiplying (25) by a.

We generate values of $WT_w(u)$ for a number of test functions w and examine the average magnitude. As alluded to previously, the result of the test (24) is that for solution candidate functions derived from our algorithm for $2 \leq p < \frac{2n}{n-2}$ and for $p = 1$, we have $WT_w(u)$ very close to zero, meaning that we can be confident that we have found appropriate solutions. However, in the cases $1 < p < 2$, $WT_w(u)$ is approximately 10 orders of magnitude larger and of a similar magnitude to $WT_w(f)$, where f is a randomly chosen function. This confirms that the algorithm does not work for the cases $1 < p < 2$, as anticipated.

10.3 Unit Square

The next domain to investigate will be the unit square. This domain was chosen because Choi and McKenna [3] solved (1) for the case $p = 4$ on this domain and so we can attempt to replicate their result to build confidence in our methods. For nonlinear cases, the initial guess is set to $u_{guess} = 20sin(\pi x)sin(\pi y)$ as proposed by Choi and McKenna.

In Fig. 5 below we see a depiction of the solution for the case $p = 4$.

Fig. 5: Solution on the Unit Square for $p = 4$

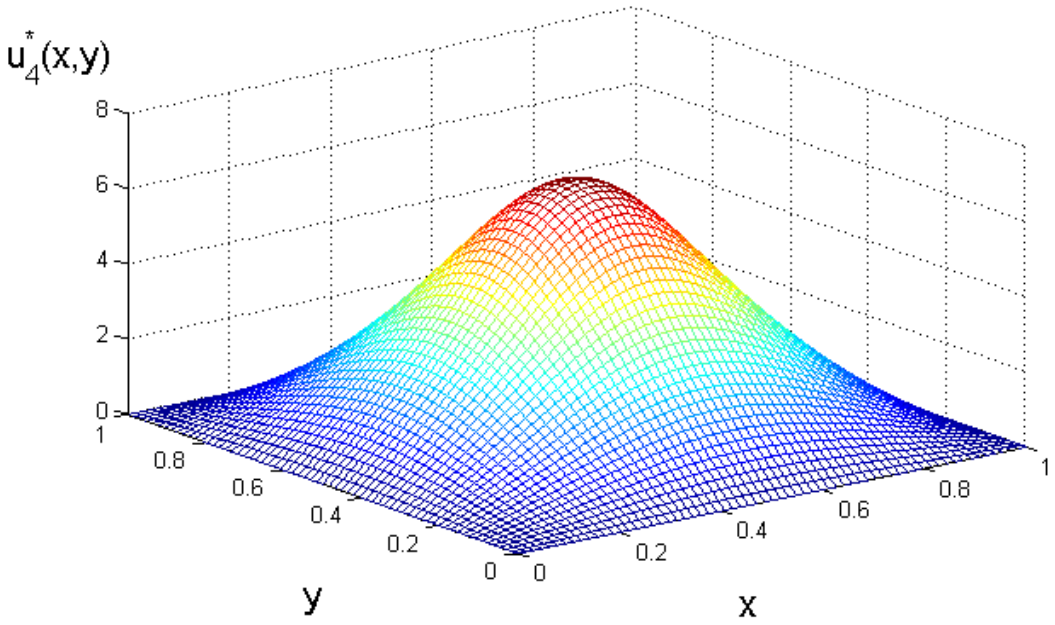

The maximum value of u_4^* is 6.62 , which matches very closely the result of 6.61 achieved by Choi and McKenna, giving additional confidence in our methods.

We recall that for the case $n = 2$, there is no restriction on the values that p can assume besides of course $p \geq 1$. We plot the solution for $p = 8$ in Fig. 6 below.

Fig. 6: Solution on the Unit Square for $p = 8$

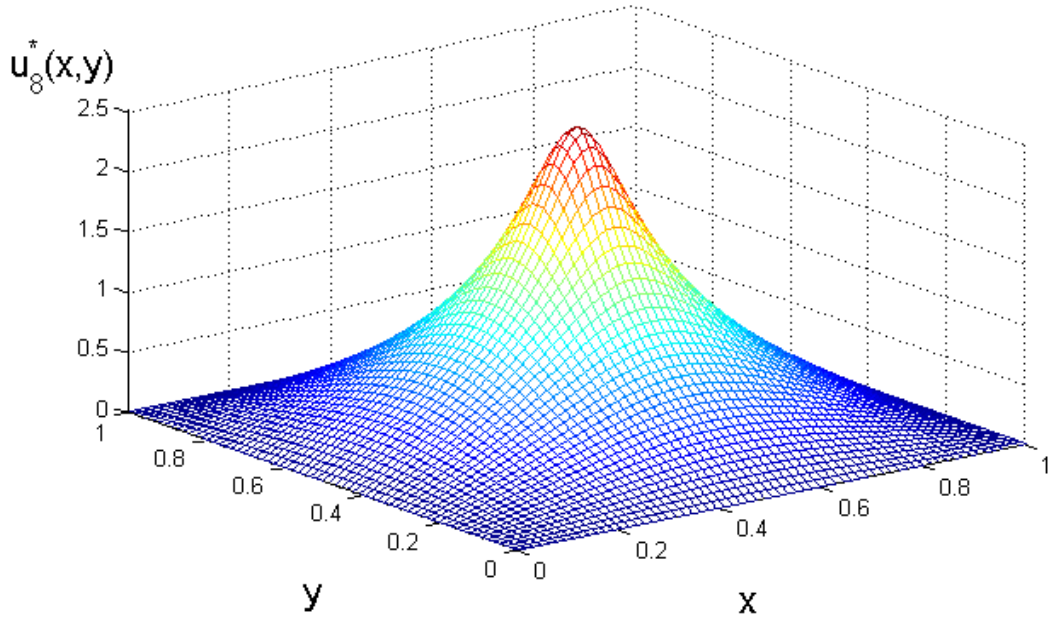

We again see good visual evidence that the hypothesis $p < q \Rightarrow \mu_{p,\Omega}(t) > \mu_{q,\Omega}(t)$ might hold true, the bulk of the solution concentrating towards the centre of the domain as p gets larger. Plotting the distribution functions (see Fig. 7) for several values of p gives further evidence to this end,

Fig. 7: Distribution Functions for Solutions on the Unit Square

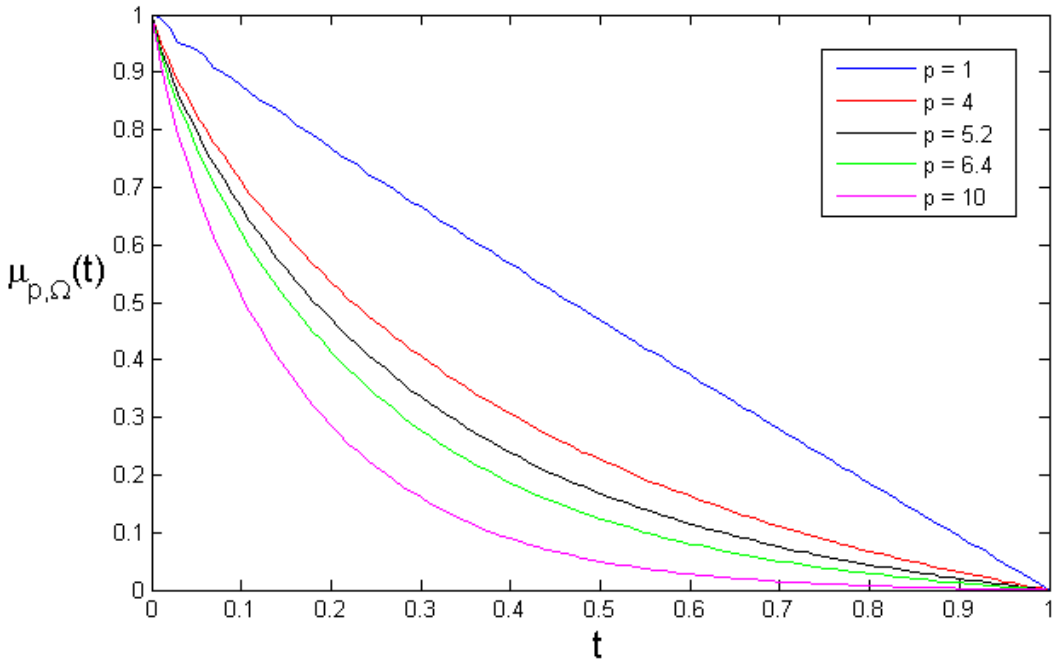

Since we are dealing with the plane ($n = 2$), p can assume any value greater or equal to 1. There is thus no critical p value at which we would expect the distribution functions to collapse toward a function negligible outside of a small neighbourhood of 0 as in the case of the ball. We again include a plot (see Fig. 8) of the behaviour of $C_p(\Omega)$ with respect to p for the unit square:

Fig. 8: Behaviour of $C_p(\Omega)$ with varying p on the Unit Square

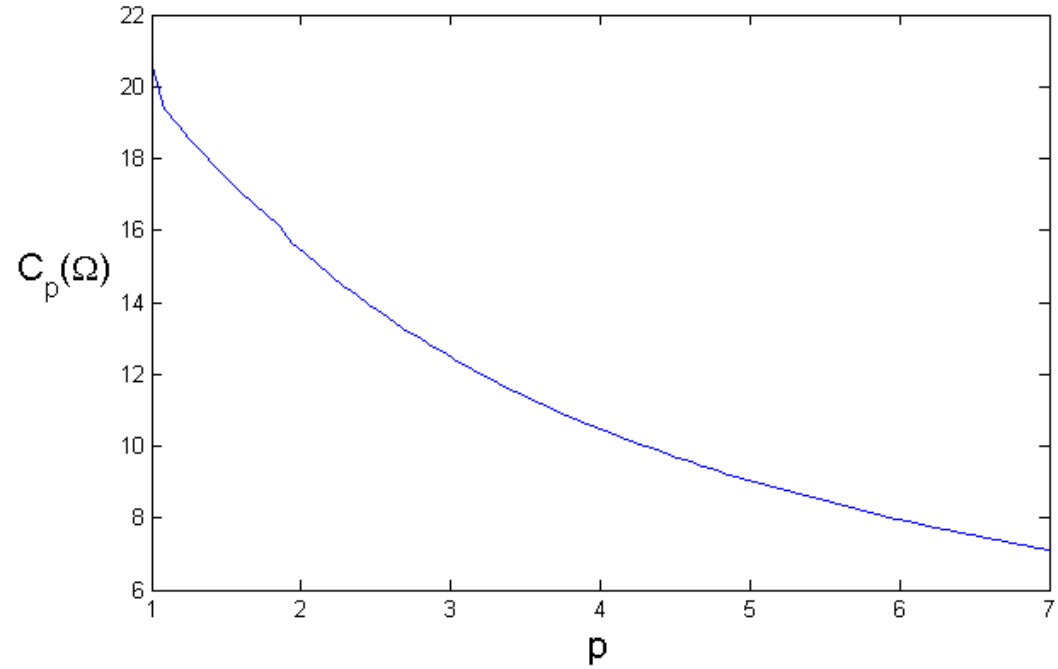

10.3.1 Numerical Verification of Results on the Unit Square

A similar procedure is used as for the unit ball to verify results numerically. This time we define

$$WT_w(u) := \int_\Omega [-\nabla u(x)\nabla w(x) + w\Lambda u(x)^{p-1}]dx \tag{26}$$

and again compute $WT_w(u)$ for our candidate solutions, with appropriate rescalings as described previously. We have already closely matched the result of Choi and McKenna for the case $p = 4$, which means that we should be able to use the value $WT_w(u_4^*)$ as a gauge for how close to zero $WT_w(u)$ should be for appropriate solutions. Again we find that for $2 \leq p < \frac{2n}{2-n}$ and $p = 1$ we get values of $WT_w(u)$ very close to zero and of the same magnitude as $WT_w(u_4^*)$, while for $1 < p < 2$ we get $WT_w(u)$ values many orders of magnitude higher. We accept the solutions for $2 \leq p < \frac{2n}{2-n}$ and $p = 1$ and reject those for $1 < p < 2$.

10.4 Rectangle of length 4 and unit width

The equation was next solved on a rectangle of length 4 and of unit width. Fig. 9 shows a plot of the solution for $p = 2.5$

Fig. 9: Solution on a Rectangle for $p = 2.5$

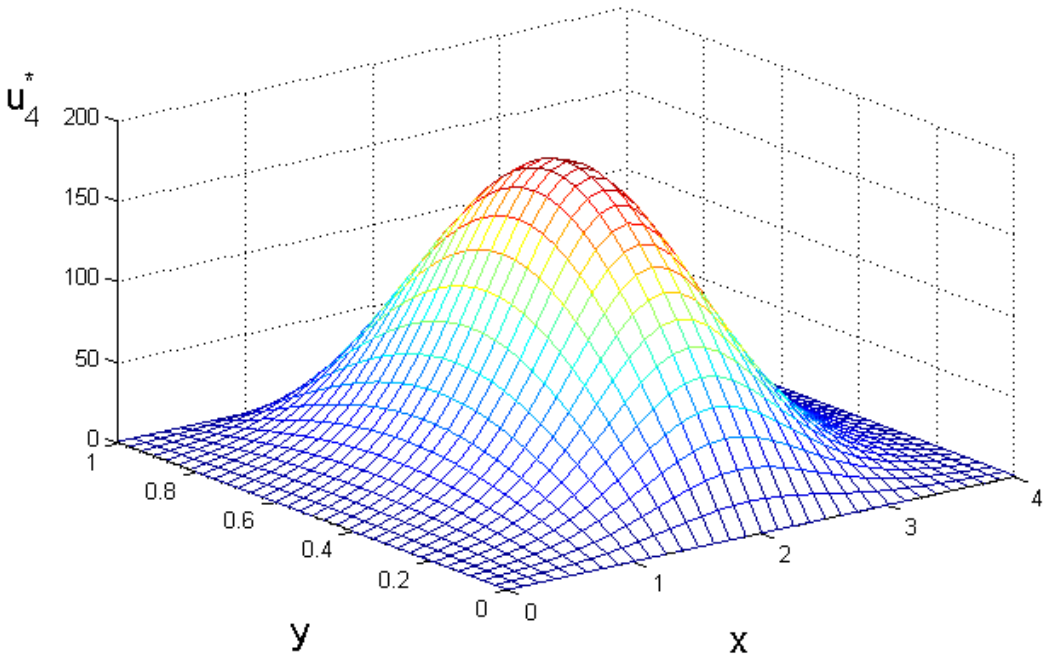

We see that the solution is bulkier across sections parallel to the y axis than it is across sections parallel to the x axis. This phenomenon becomes more extreme with larger p values, as can be seen from the solution for $p = 5$ in Fig. 10.

Fig. 10: Solution on a Rectangle for $p = 5$

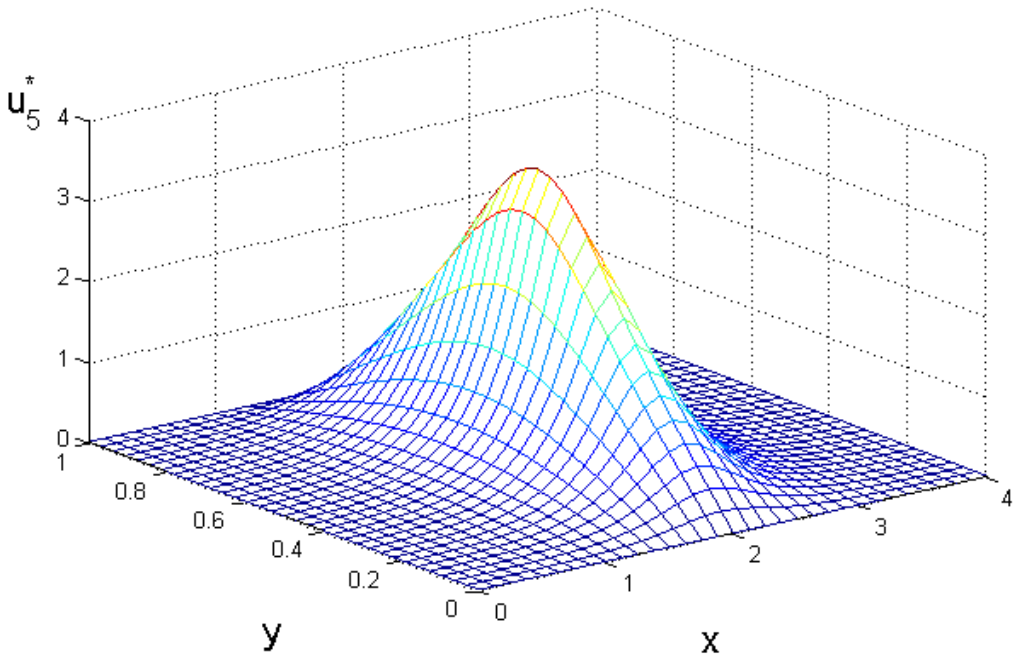

This behaviour may seem strange, however a numerical test of whether the function solves the problem weakly similar to that performed on the unit square confirms that these are indeed solutions. Moreover, we find the desired behaviour of the distribution functions corresponding to the conjecture as can be seen in Fig. 11.

Fig. 11: Distribution Functions for Solutions on the Rectangle

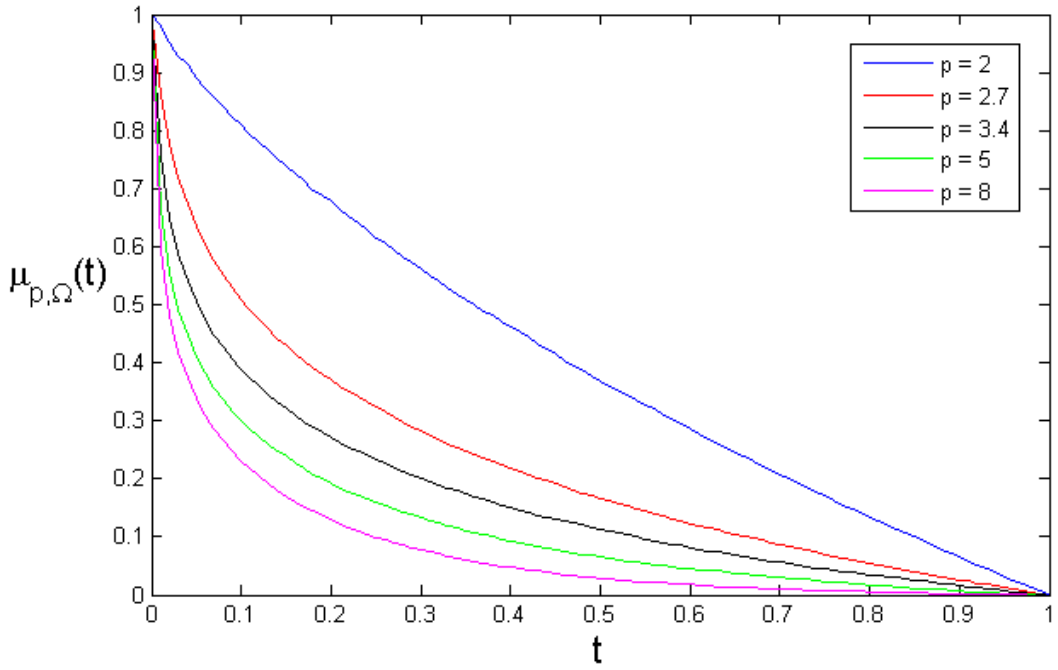

Fig. 12 shows a plot of the values of the constant $C_p(\Omega)$ for the rectangle.

Fig. 12: Behaviour of $C_p(\Omega)$ with varying p on the Rectangle

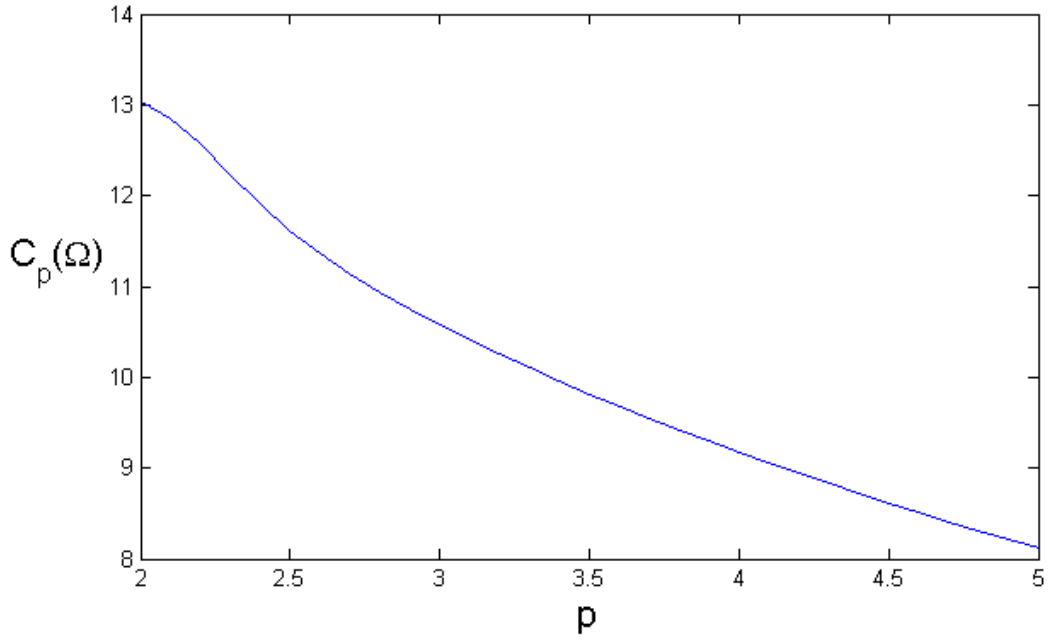

11 Conclusion

We have developed the theoretical background to design a numerical investigation of the constant $C_p(\Omega)$ by drawing on both classical and modern results.

The Sobolev Imbedding Theorem as well as the Rellich-Kondrachov Compactness Theorem were indispensable in proving the existence of solutions that achieve the minimisation of the functional $\phi_p(u)$. Algorithms developed by Choi and McKenna, and Li and Zhou were inspired by the important work done by Ambrosetti and Rabinowitz in developing the Mountain Pass Theorem.

Although we set out to find solutions to (1) for all permissible values of p, being $1 \leq p < \frac{2n}{n-2}$ for $n \geq$ and $p \geq 1$ for $n = 2$, the Li- Zhou algorithm we employ does not work for $1 < p < 2$. However, the results we obtain for all other permissible values of p give solutions that hold under both numerical and analytical verifications, for the domains of the unit ball in n dimensions, the unit square in the plane and a rectangle in the plane.

Moreover, for all values of p other than $1 < p < 2$, compelling evidence has been found for the conjecture proposed by thesis supervisor Dr Ratzkin. All of the results point towards the conclusion that

$$p < q \Rightarrow \mu_{p,\Omega}(t) \geq \mu_{q,\Omega}(t) \; \forall t \in [01]$$

should be true for the domains that have been investigated, and therefore may even hold more generally.

The question of the truth of this conjecture thus warrants further investigation. One could go on to analyse more general domains and develop a working algorithm for the cases $1 < p < 2$, while there is hope of one day finding a rigorous analytical proof.

References

[1] Antonio Ambrosetti and Paul H Rabinowitz. Dual variational methods in critical point theory and applications. *Journal of functional Analysis*, 14(4):349–381, 1973.

[2] Tom Carroll and Jesse Ratzkin. Interpolating between torsional rigidity and principal frequency. *Journal of Mathematical Analysis and Applications*, 379(2):818–826, 2011.

[3] Yung Sze Choi and P Joseph McKenna. A mountain pass method for the numerical solution of semilinear elliptic problems. *Nonlinear Analysis: Theory, Methods & Applications*, 20(4):417–437, 1993.

[4] Jacob Fish and Ted Belytschko. *A first course in finite elements*. Wiley. com, 2007.

[5] Basilis Gidas, Wei-Ming Ni, and Louis Nirenberg. Symmetry and related properties via the maximum principle. *Communications in Mathematical Physics*, 68(3):209–243, 1979.

[6] David Autor Gilbarg and Neil S Trudinger. *Elliptic partial differential equations of second order*, volume 224. Springer, 2001.

[7] Yongxin Li and Jianxin Zhou. A minimax method for finding multiple critical points and its applications to semilinear pdes. *SIAM Journal on Scientific Computing*, 23(3):840–865, 2001.

[8] Zeev Nehari. On a class of nonlinear second-order differential equations. *Transactions of the American Mathematical Society*, 95(1):101–123, 1960.

[9] Wei-Ming Ni. Recent progress in semilinear elliptic equations (solutions for nonlinear elliptic equations). *in RIMS Kokyuroku, Kyoto University, Kyoto, Japan*, 679:1–39, 1989.

[10] Jesse Ratzkin. Eigenvalues of euclidean wedge domains in higher dimensions. *Calculus of Variations and Partial Differential Equations*, 42(1-2):93–106, 2011.

[11] Friedrich Sauvigny. *Partial differential equations 1 & 2. Universitext*. Springer, Berlin (2003/2004), 2003.